JACS
JOURNAL OF THE AMERICAN CHEMICAL SOCIETY
pubs.acs.org/JACS
Article

Data-Driven Insight into the Reductive Stability of Ion−Solvent Complexes in Lithium Battery Electrolytes

Yu-Chen Gao, Nan Yao, Xiang Chen,* Legeng Yu, Rui Zhang, and Qiang Zhang

Cite This: J. Am. Chem. Soc. 2023, 145, 23764−23770
Read Online

ABSTRACT: Lithium (Li) metal batteries (LMBs) are regarded as one of the most promising energy storage systems due to their ultrahigh theoretical energy density. However, the high reactivity of the Li anodes leads to the decomposition of the electrolytes, presenting a huge impediment to the practical application of LMBs. The routine trial-and-error methods are inefficient in designing highly stable solvent molecules for the Li metal anode. Herein, a data-driven approach is proposed to probe the origin of the reductive stability of solvents and accelerate the molecular design for advanced electrolytes. A large database of potential solvent molecules is first constructed using a graph theory-based algorithm and then comprehensively investigated by both first-principles calculations and machine learning (ML) methods. The reductive stability of 99% of the electrolytes decreases under the dominance of ion−solvent complexes, according to the analysis of the lowest unoccupied molecular orbital (LUMO). The LUMO energy level is related to the binding energy, bond length, and orbital ratio factors. An interpretable ML method based on Shapley additive explanations identifies the dipole moment and molecular radius as the most critical descriptors affecting the reductive stability of coordinated solvents. This work not only affords fruitful data-driven insight into the ion−solvent chemistry but also unveils the critical molecular descriptors in regulating the solvent's reductive stability, which accelerates the rational design of advanced electrolyte molecules for next-generation Li batteries.

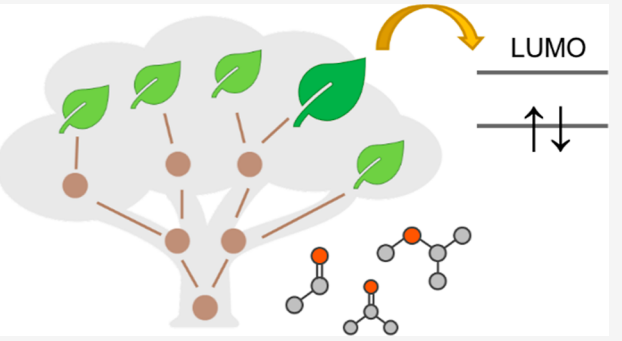

INTRODUCTION

The emergence of rechargeable batteries has revolutionized modern technology, catalyzing the development of large-scale grids and myriad consumer electronics such as smartphones, laptops, and electric vehicles.[1−3] Especially lithium (Li) ion batteries (LIBs), one of the most widely applied rechargeable batteries, have significantly altered patterns of energy consumption and lifestyle habits.[4−7] Although LIBs have dominated the rechargeable battery market for years due to their obvious advantages, their practical energy density is approaching the theoretical limits. As a result, next-generation high-energy-density batteries are strongly required due to the increasing demands from modern society.[8−11]

Li metal batteries (LMBs) have emerged as promising energy storage devices by surpassing the limitations of current LIBs due to their ultrahigh theoretical capacity (3860 mAh g^{-1}) and the very negative electrochemical potential (−3.04 V vs the standard hydrogen electrode) of the Li metal anode.[12−14] However, most electrolytes including the ester-based electrolytes widely adopted in LIBs are unstable against highly reactive and low-potential Li metal anodes, which seriously impedes the practical application of LMBs.[15,16] Specifically, the continuous interfacial reactions can induce the decomposition of the electrolytes and the corrosion of working Li metal anodes, which induce rapid capacity decay and a short cycling lifespan.[17−19] Moreover, solvents decompose to generate and accumulate flammable gases, which causes serious safety hazards.[20,21] Routine electrolyte recipes have yet to bring about revolutionary improvements for LMBs. To overcome these challenges and unlock the full potential of LMBs, it is crucial to propose novel electrolyte design strategies and explore new solvent molecules to establish stable interfaces between the electrolytes and anodes.[22,23]

Several electrolyte components (including Li salts, solvents, and additives) have been formulated to achieve good compatibility with Li metal anodes through extensive experimentation.[24−27] However, this trial-and-error approach is always time-consuming, and the underlying electrolyte chemistry at the atomic level is far from clear.[28] Recently, the ion−solvent complex model has inspired new insights into electrolyte design and demonstrated significant success in rechargeable batteries.[29,30] Specifically, the ion−solvent complexes have a much lower energy level of the lowest unoccupied molecular

Received: August 2, 2023
Published: September 13, 2023

https://doi.org/10.1021/jacs.3c08346
J. Am. Chem. Soc. 2023, 145, 23764−23770

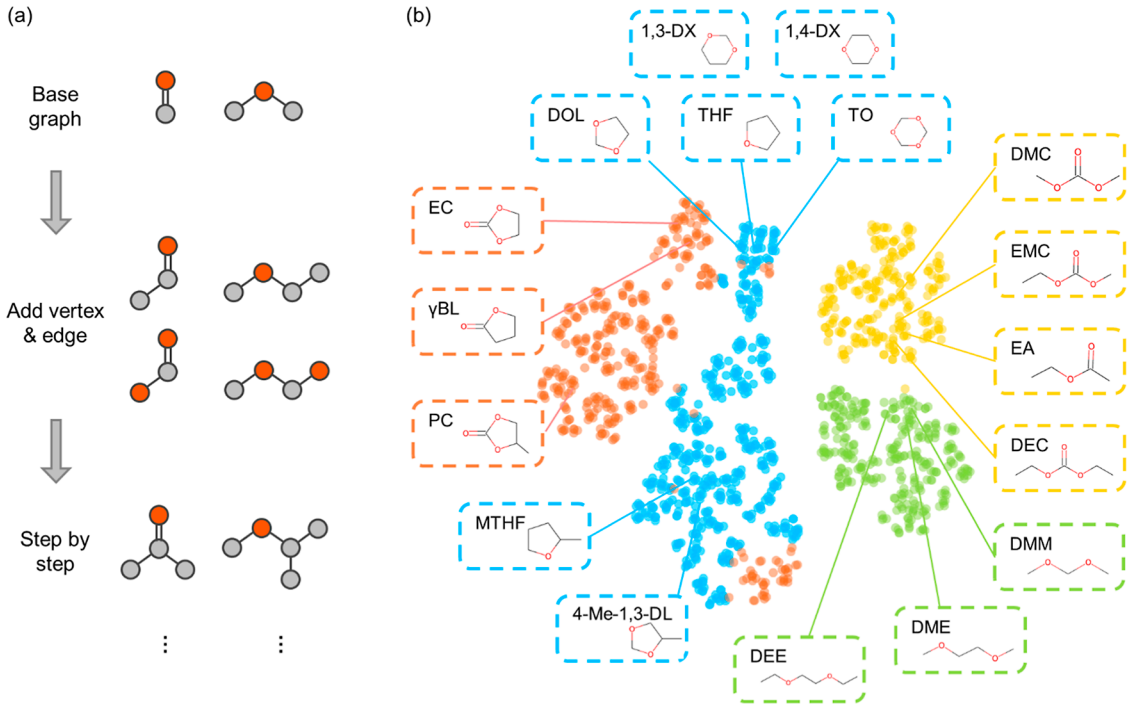

Figure 1. Generation and visualization of the solvent molecular database. (a) Graph-based algorithm for generating solvent molecules. Carbon and oxygen atoms are marked with gray and red, respectively. (b) Visualization of the solvent molecular database based on a clustering method. Each point represents a molecule. The linear carbonyl compounds, cyclic carbonyl compounds, linear ethers, and cyclic ethers are marked with yellow, red, green, and blue, respectively.

orbital (LUMO) than pure solvents. As a result, the solvents in the solvation shell of Li ions are prone to decompose, leading to the instability of the electrolyte−anode interface.[31] Although the new model has unveiled the obscure role of ion−solvent complexes in regulating the reductive stability of routine electrolytes, previous studies have primarily focused on investigating the interactions between different metal cations and limited solvents. It is crucial to conduct a comprehensive investigation of the interaction relationships between Li ions and a large quantity of solvent molecules, which is beneficial to designing new electrolyte solvents through a highly efficient data-driven approach.

Thanks to the rapid advancement of computer science, machine learning (ML) methods have become increasingly convenient for extracting knowledge from numerous solvent molecules.[32−36] In particular, the development of interpretable ML has transformed the research paradigm from purely data-driven to knowledge discovery with strong interpretability.[37,38] A typical interpretable algorithm, Shapley additive explanations (SHAP), employs game theory to enhance the analysis of the relative importance of each variable in ML predictions.[39,40] By leveraging ML and interpretable analysis, it becomes possible to explore the relationship between the stability of ion−solvent complexes and intrinsic molecular properties and structural characteristics, thereby providing valuable insights for electrolyte design.

In this contribution, a data-driven approach is proposed to probe the origin of the reductive stability of numerous Li battery electrolyte solvents by combining first-principles calculations and ML models. Graph theory algorithms were applied to generate a large solvent molecular database, which was further comprehensively studied by density functional theory (DFT) calculations based on ion−solvent complex models. A positive and approximately linear relationship was observed between the reduction in both the highest occupied molecular orbital (HOMO) and LUMO energy levels and the binding energy. Furthermore, both the dipole moment (μ) and the molecular radius (R) were identified as the most significant descriptors affecting the reductive stability of coordinated solvent molecules, according to the SHAP interpretable ML analysis. This work affords an in-depth insight into the origin and rules underlying stability variation of ion−solvent complexes, paving the way for rapid screening of solvents and accelerating the design of advanced electrolytes for LMBs.

RESULTS AND DISCUSSION

Solvents play a crucial role in determining the stability of electrolytes and the cycling lifespan of batteries.[41−44] The emergence of new solvent molecules has exhibited great potential in enhancing battery performance.[45−47] To facilitate a comprehensive analysis of solvents, constructing a large solvent molecular database is imperative. A graph-based algorithm (Figure 1a and Table S1) was first proposed for constructing the database. Solvent molecules are viewed as graphs, with atoms (carbon and oxygen) as vertices and bonds (single and double bonds) as edges. Since ethers and carbonyl compounds are widely used as electrolyte solvents, the graph-based algorithm generates molecules starting from two basic molecules (formaldehyde and dimethyl ether) and iteratively adds vertices and edges to generate potential solvent molecules until the molecules include nine heavy atoms (including carbon and oxygen atoms). Besides, molecules containing active hydrogen atoms (i.e., alcohols and acids) were excluded during generation due to their high reactivity with Li metal anodes. As a result, the database comprises a total of 1399 solvent molecules, including 44.9% carbonyl compounds and 55.1% ethers. The

https://doi.org/10.1021/jacs.3c08346
J. Am. Chem. Soc. 2023, 145, 23764−23770

negative formation energy of all solvent molecules indicates the rationality of the generated solvent molecules (Figure S1).

To visually present the database, the molecules are clustered by combining the extended-connectivity circular fingerprints[48] and the t-distributed stochastic neighbor embedding (t-SNE) method[49] (Figure 1b). The t-SNE algorithm maps similar molecules to neighboring points in 2D space. All 1399 molecules are divided into four categories: linear carbonyl compounds (yellow), cyclic carbonyl compounds (red), linear ethers (green), and cyclic ethers (blue). The four regions are almost clearly separated from each other, which demonstrates the effectiveness of the clustering method.

Due to the completeness of the generation algorithm, all routine solvent molecules that conform to the rules are included in the database. For instance, widely applied solvent molecules, such as dimethyl carbonate, ethylene carbonate, 1,2-dimethoxyethane (DME), and 1,3-dioxolane (DOL), have been identified in these four regions. Furthermore, the recently reported 1,3,5-trioxane (TO) was found within the neighborhood of the classic solvent molecule DOL. Assisted by the electrolyte containing mixed solvents of TO and DME, a Li metal pouch cell of 440 W h kg^{-1} achieves a lifespan of 130 cycles, which exhibits potential for long-cycling and high-energy-density LMBs.[50] Additionally, 1,3-dioxane (1,3-DX) and 1,4-dioxane (1,4-DX), which are also located near DOL, have been reported as weakly solvating solvents capable of significantly modulating the competitive interactions between anions, solvents, and Li ions.[51] Consequently, the clustering results reveal the potential structural similarities and differences among the promising solvent molecules, which afford a promising approach to screening advanced electrolyte molecules.

The first-principles calculations were performed for all 1399 solvent molecules to comprehensively investigate the origin of the reductive stability of electrolytes. In comparison to pure solvents, the majority of solvents coordinated with the Li ion exhibit a lower LUMO energy level (Figure 2a), which indicates

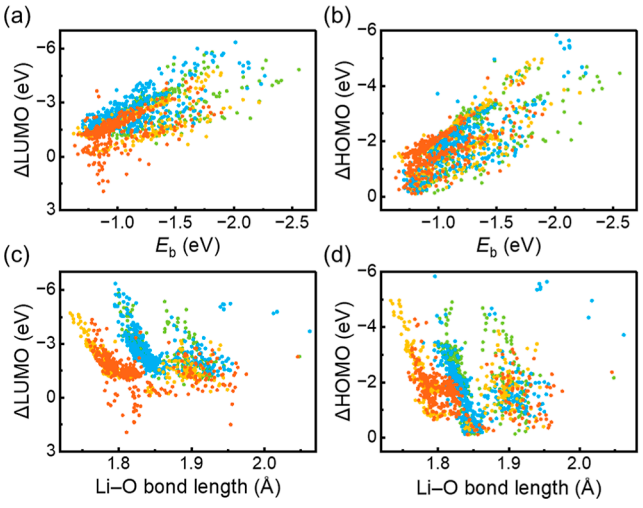

Figure 2. Correlation between HOMO and LUMO energy level changes and binding energy as well as Li−O bond length. Correlation between the (a) LUMO and (b) HOMO energy level changes and binding energy (E_b). Correlation between the (c) LUMO and (d) HOMO energy level changes and Li−O bond length. Molecular color mapping remains the same as that in Figure 1. The linear carbonyl compounds, cyclic carbonyl compounds, linear ethers, and cyclic ethers are marked with yellow, red, green, and blue, respectively.

a decreased reductive stability of solvents when they are coordinated with Li ions. Besides, a more obvious decrease in the LUMO energy level is observed for ether molecules, especially the cyclic ones, than carbonyl compounds (−6 to −2 eV vs −3 to 0 eV). However, it is noteworthy that 1% of solvent molecules deliver an increased LUMO energy level. These molecules are all six-membered lactones and their elevated LUMO energy levels are attributed to the conjugated structure and the low ring strain in the six-membered ring (Figure S2). Additionally, the HOMO energy level of all solvent molecules also dropped (Figure 2b), indicating enhanced oxidation stability of the coordinated solvents.

A positive linear correlation is observed between the LUMO and HOMO energy level changes and the binding energy of a Li ion and a solvent (Figure 2a,b). Generally, the larger the change in the binding energy, the more electrons are transferred from the solvent molecules to the Li ions (Figure S3). The bond length analysis further substantiates these observations. Ion−solvent complexes indicate that Li ions prefer to bind with oxygen atoms of the ether and carbonyl solvent molecules, such as the carbonyl oxygen in carbonyl molecules. As a result, the Li−O bond length has a certain linear correlation with changes in both the LUMO and HOMO energy levels (Figure 2c,d). Specifically, the shorter the Li−O bond length in coordinated solvents, the larger the bond energy and the stronger the interaction with Li ions. Moreover, most carbonyl molecules exhibit a Li−O bond length that is shorter than that of ether molecules, which is more pronounced in solvent molecules containing only one oxygen atom (Figure S4). This phenomenon can be attributed to the more negative charge on the carbonyl oxygen, which results in a stronger interaction with the Li ion. Besides, the C−O bond length increases after binding with a Li ion, indicating the weakening of C−O bonds and reduced reductive stability of the ion−solvent complexes (Figure S5a,b). Particularly in solvent molecules containing only one oxygen atom, a positive linear relationship is observed between the changes in the C−O bond length and the LUMO energy level change (Figure S5c,d).

The binding energy, Li−O bond length, and changes in C−O bond length maintain excellent coherence in their relationships with the LUMO energy level change, all suggesting that forming ion−solvent complexes generally decreases the reductive stability of working electrolytes. The composition of LUMO is further analyzed to unveil the origin of the reduced reductive stability of ion−solvent complexes. Specifically, the LUMO of ion−solvent complexes is primarily constituted by the 2p orbitals of carbon and oxygen atoms. An approximately linear relationship was found between the ratio of carbon 2p orbitals in the LUMO and the LUMO energy level changes (Figure S6). The Li ion attracts electrons from the oxygen atom and thus increases the contribution ratio of carbon in the LUMO, leading to a reduction in the LUMO energy level. Moreover, there are obvious differences between the ether and carbonyl molecules. On the one hand, the linear trend in ether molecules is not as significant as that in carbonyl molecules, which is due to the different electronic structures of oxygen atoms when the Li ion interacts with the ether oxygen and the carbonyl oxygen, respectively (Figure S7). On the other hand, the contribution ratio of carbon in the LUMO in carbonyl molecules is generally higher than that in ether molecules. This is attributed to the stronger electron-withdrawing effect of the carbonyl oxygen compared to that of the ether oxygen, which results in more electrons being attracted to the Li ion and a higher ratio of

https://doi.org/10.1021/jacs.3c08346
J. Am. Chem. Soc. 2023, 145, 23764−23770

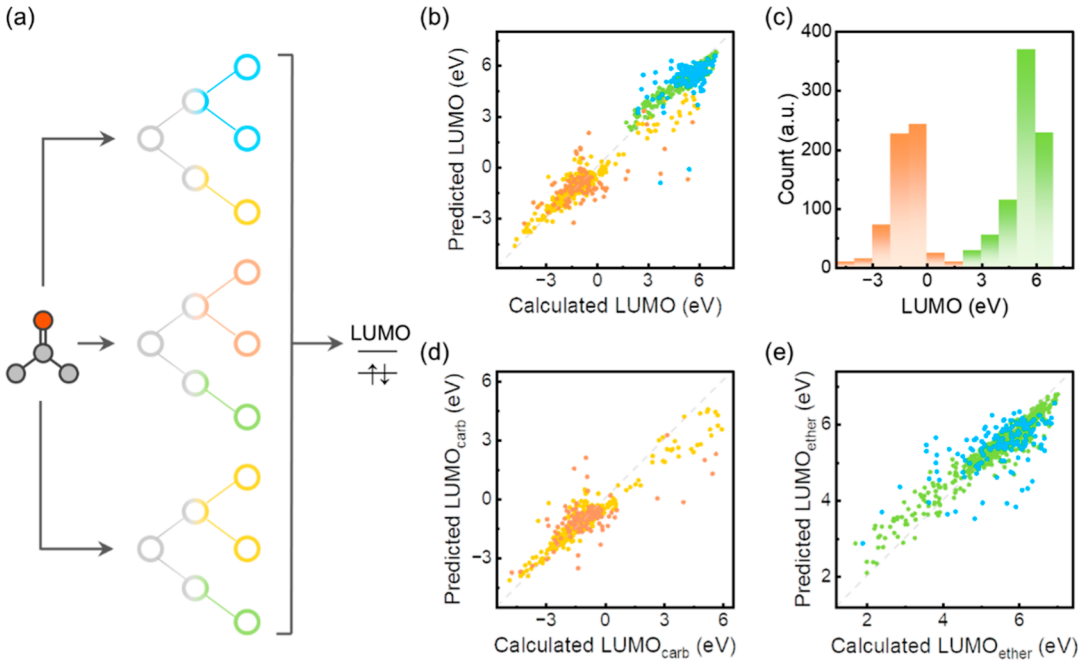

Figure 3. Prediction of LUMO energy levels of ion−solvent complexes. (a) Schematic diagram of the random forest (RF) model. (b) Results of RF model prediction for all 1399 molecules. (c) Distribution of LUMO energy levels of ion−solvent complexes. Carbonyl compounds and ethers are mainly included in the red and green bars, respectively. (d) Results of RF model prediction for carbonyl compounds. (e) Results of RF model prediction for ethers. Training set is marked with yellow or green. Test set is marked with red or blue.

carbon. The orbital analysis connects the LUMO energy level changes with the ratio of carbon 2p orbitals, deepening the understanding of the reductive stability of ion−solvent complexes.

The stability of the majority of electrolytes is predominantly governed by ion−solvent complexes; therefore, analyzing them deeply holds significant implications for the rational design of electrolyte molecules. Taking dimethoxymethane (DMM) as a benchmark, 246 molecules possess higher LUMO energy levels than DMM (Figure S8). However, the LUMOs of these molecules all fall below those of DMM after forming ion−solvent complexes, which indicates that the LUMO of ion−solvent complexes is a key point to focus on.

To delve deeply into the intrinsic relationship between the LUMO energy levels of ion−solvent complexes and solvent molecular characteristics, the number of carbonyl oxygens (#(═O)), μ, R, molecular weight (Molwt), the number of rings (Ring), the number of branches (Bran), the ratio of carbon atoms to oxygen atoms (#C/#O), average electronegativity (Avg X), and average ionization energy (Avg I) were extracted to describe the molecules (Table S2). Among these, #(═O) is a significant descriptor to distinguish between ether and carbonyl molecules. The μ reflects the separation of positive and negative charge centers and, thus, is used to measure molecular polarity. The R and Molwt describe the size of the molecules from the perspectives of volume and mass, respectively, and the Ring and Bran describe the structural features of the molecules. The #C/#O reflects the ratio of elements within the molecule. The Avg X and Avg I represent the electronic properties of each atom at the molecular level.

In order to select important and rational features from the above descriptors, the Pearson correlation coefficient was applied to discover the features potentially in high correlation with the LUMO energy level, which also helps to reduce the correlation between the features to a certain extent. According to the heatmap of variable correlation (Figure S9), #(═O), μ, R, Avg X, Bran, and #C/#O were ultimately selected as molecular feature descriptors for the following ML investigations.

Ten ML algorithms (Table S3) were utilized to predict the LUMO energy levels of 1399 coordinated solvent molecules, among which the random forest (RF) model (Figure 3a) delivers the best performance with a mean absolute error (MAE) of 0.68 eV (Figure 3b) and reaches state-of-the-art results through 4-fold cross-validation (Table S4). The majority of test data points are close to the line of perfect prediction, and their distribution is similar to that of the training data points. Ether and carbonyl molecules are divided into two regions, which can be validated from their varied LUMO energy level distributions (Figure 3c). Three feature importance ranking methods have proven that #(═O) is the most impactful feature (Table S5), which aligns well with the difference in LUMO energy levels between ether and carbonyl molecules due to the electronic structures of the oxygens. In addition, μ and R play critical roles in predicting the LUMO energy levels, while the contribution of #C/#O is minor.

Given the substantial differences between ether and carbonyl molecules, ML models were built for these two types of molecules to better understand the factors influencing their LUMO energy levels. Following feature selection, μ, R, Bran, Molwt, Avg X, and Ring were chosen as molecular descriptors to input into the models. After model comparison, the RF model still achieves the best performance (Tables S6 and S7). The MAE values for carbonyl and ether molecules are 0.68 and 0.53 eV, respectively. The test data points were relatively close to the prediction line, indicating a good prediction performance (Figure 3d,e).

The SHAP was combined with the trained model to improve its interpretability and observe the influence of each molecular feature on the LUMO energy level of coordinated solvents (Figure 4a). For a single feature, the vertical distribution reflects

https://doi.org/10.1021/jacs.3c08346
J. Am. Chem. Soc. 2023, 145, 23764−23770

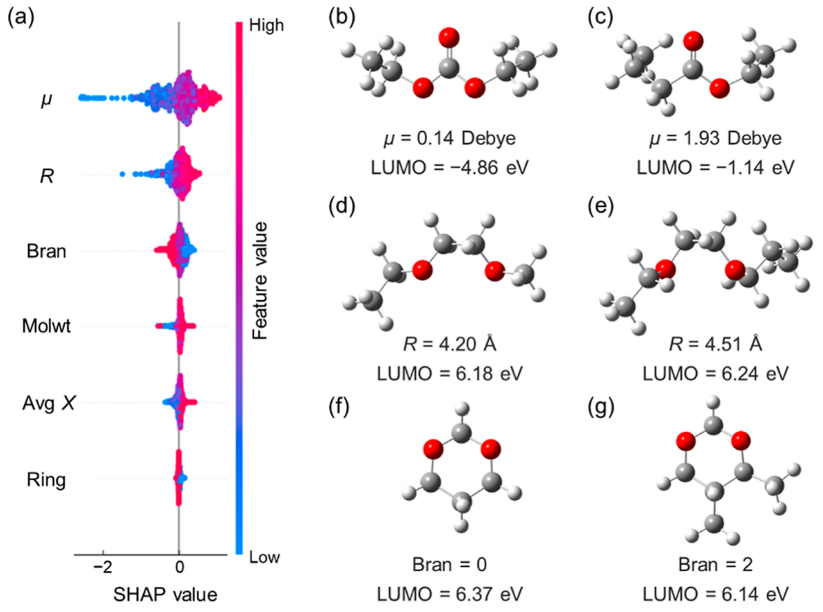

Figure 4. Interpretable ML for predicting LUMO energy levels of ion−solvent complexes. (a) Shapley features a ranking for ethers. SHAP value means the contribution of the sample point to the model's performance. Geometric structures of (b) diethyl carbonate (DEC), (c) ethyl butyrate (EB), (d) 1-ethoxy-2-methoxyethane, (e) 1-(2-ethoxyethoxy)propane, (f) 1,3-dioxane (1,3-DX), and (g) 4,5-dimethyl-1,3-dioxane molecules. The hydrogen, carbon, and oxygen atoms are marked with white, gray, and red, respectively.

the number of molecules and the horizontal direction reflects the contribution of the molecular feature values to the prediction results. In both ether and carbonyl molecules, μ has the most significant impact on the LUMO energy level, which is consistent with the prediction results for all molecules (Figure 4a and Tables S8 and S9). Specifically, a smaller μ (0 to 3 D) has a greater impact on the LUMO energy level, and it has shown a certain positive correlation with the LUMO energy level. For instance, the diethyl carbonate (DEC) molecule has a low μ value (0.14 D) due to its structural symmetry (Figure 4b). If one of the ether oxygen atoms is replaced with a carbon atom, forming the ethyl butyrate (EB) molecule, μ becomes 1.93 D (Figure 4c). Consequently, the LUMO energy level of the coordinated molecule rises dramatically from −4.86 to −1.14 eV. A large μ indicates a high degree of separation between the positive and negative charge centers within a molecule, reflecting the high molecular polarity. Then, statistically, a great shielding effect against the external field is created for numerous molecules, which corresponds to a high dielectric constant for the solvents. The relationship between the μ and the solvent dielectric constant can be observed (Figure S10), and the Spearman value equals 0.53 (larger than 0.3), indicating a positive correlation between these two properties. The high dielectric constant in the solvents implies weak binding with Li ions (Figure S11), which indicates less charge transfer from the solvent molecules to the Li ions, leading to less reduction in the LUMO energy level. Therefore, μ is an important descriptor in describing the reductive stability of electrolyte solvents.

Beyond μ, R and Bran also influence the reductive stability of the coordinated solvents to some extent (Figures 4a and S12). Using ether-based molecules as an example, the SHAP indicates a positive correlation between R and the contribution to the prediction of the LUMO energy level, while Bran exhibits a negative correlation. However, most molecules are concentrated near a SHAP value of zero, indicating their limited impact on the LUMO energy level. By selecting molecules with similar μ, it was found that extending the carbon chain increases R, which results in an elevation of the LUMO energy level (Figure 4d,e). Conversely, adding branches to the 1,3-DX molecule leads to a decrease in the LUMO energy level (Figure 4f,g).

The application of ion−solvent complex theory and interpretable ML in electrolyte solvent molecules holds great significance for understanding the factors that influence the reductive stability of electrolytes and designing advanced electrolyte molecules. First, a molecule generation algorithm based on graph theory has been developed to construct a complete database of electrolyte solvent molecules under specific rules. Its completeness and portability guide the development of molecular databases for various scenarios. Second, the ion−solvent complex model demonstrates excellent applicability in a wide molecular space where 99% of molecules deliver reduced LUMO energy after interacting with Li ions. Besides, the change in the LUMO energy level is well correlated with the binding energy, bond length, and ratio of carbon 2p orbitals in the LUMO. Third, the application of interpretable ML has unearthed the intrinsic connection between the LUMO energy level of ion−solvent complexes and the characteristics of solvent molecules. The μ and R serve as important descriptors to describe the reductive stability of electrolyte solvent molecules. Therefore, molecular polarity should be taken into account during molecular design and high-throughput screening for developing new electrolytes.

CONCLUSIONS

The reductive stability of ion−solvent complexes in Li battery electrolytes has been comprehensively investigated by combining DFT calculations and ML models. A large database with 1399 solvent molecules is built using the novel graph-based algorithm. After coordination with a Li ion, 99% of the solvents deliver a reduced LUMO energy level. The LUMO energy change exhibits a positive correlation with the binding energy, Li−O bond length, and C−O bond length. The essence of the LUMO energy level changes can be attributed to the contribution ratio of carbon 2p orbitals in the LUMO. The

https://doi.org/10.1021/jacs.3c08346
J. Am. Chem. Soc. 2023, 145, 23764−23770

RF model delivers the best performance in predicting the LUMO energy level among the ten routine ML models. SHAP analysis based on the RF model further reveals that μ and R are the most significant features in regulating the LUMO energy level. This work probes the reductive stability of ion−solvent complexes through a data-driven approach and unveils the essential factors influencing the reductive stability of electrolytes, which affords great theoretical references for the rational design of advanced electrolyte molecules.

■ ASSOCIATED CONTENT

Supporting Information

The Supporting Information is available free of charge at https://pubs.acs.org/doi/10.1021/jacs.3c08346.

Complete molecular generation algorithm, calculation methods, and ML details (PDF)

Database of all 1399 constructed solvent molecules (XLSX)

■ AUTHOR INFORMATION

Corresponding Author

Xiang Chen − *Beijing Key Laboratory of Green Chemical Reaction Engineering and Technology, Department of Chemical Engineering, Tsinghua University, Beijing 100084, China;* orcid.org/0000-0002-7686-6308; Email: xiangchen@mail.tsinghua.edu.cn

Authors

Yu-Chen Gao − *Beijing Key Laboratory of Green Chemical Reaction Engineering and Technology, Department of Chemical Engineering, Tsinghua University, Beijing 100084, China;* orcid.org/0000-0002-3143-4077

Nan Yao − *Beijing Key Laboratory of Green Chemical Reaction Engineering and Technology, Department of Chemical Engineering, Tsinghua University, Beijing 100084, China;* orcid.org/0000-0003-1965-2917

Legeng Yu − *Beijing Key Laboratory of Green Chemical Reaction Engineering and Technology, Department of Chemical Engineering, Tsinghua University, Beijing 100084, China;* orcid.org/0000-0002-9622-3334

Rui Zhang − *Beijing Huairou Laboratory, Beijing 101400, China;* orcid.org/0000-0003-3740-8352

Qiang Zhang − *Beijing Key Laboratory of Green Chemical Reaction Engineering and Technology, Department of Chemical Engineering, Tsinghua University, Beijing 100084, China;* orcid.org/0000-0002-3929-1541

Complete contact information is available at: https://pubs.acs.org/10.1021/jacs.3c08346

Author Contributions

Y.-C.G. and N.Y. contributed equally. All authors have given approval to the final version of the manuscript.

Notes

The authors declare no competing financial interest.

■ ACKNOWLEDGMENTS

This work was supported by the National Key Research and Development Program (2021YFB2500300), the National Natural Science Foundation of China (T2322015, 22109086, 22209093, 22209094, and 21825501), the Key Research and Development Program of Yunnan Province (202103AA080019), the Ordos-Tsinghua Innovative & Collaborative Research Program in Carbon Neutrality, and the Young Elite Scientists Sponsorship Program by CAST (2021QNRC001). The authors acknowledged the support from Tsinghua National Laboratory for Information Science and Technology for theoretical simulations. We thank Zheng Li, Yun-Wei Song, Shu-Yu Sun, and Chao Han for their helpful discussion.

■ REFERENCES

(1) Zhu, Z.; Jiang, T.; Ali, M.; Meng, Y.; Jin, Y.; Cui, Y.; Chen, W. Rechargeable Batteries for Grid Scale Energy Storage. *Chem. Rev.* **2022**, *122*, 16610−16751.

(2) Schmuch, R.; Wagner, R.; Hörpel, G.; Placke, T.; Winter, M. Performance and Cost of Materials for Lithium-Based Rechargeable Automotive Batteries. *Nat. Energy* **2018**, *3*, 267−278.

(3) Zeng, X.; Li, M.; Abd El-Hady, D.; Alshitari, W.; Al-Bogami, A. S.; Lu, J.; Amine, K. Commercialization of Lithium Battery Technologies for Electric Vehicles. *Adv. Energy Mater.* **2019**, *9*, 1900161.

(4) Harper, G.; Sommerville, R.; Kendrick, E.; Driscoll, L.; Slater, P.; Stolkin, R.; Walton, A.; Christensen, P.; Heidrich, O.; Lambert, S.; Abbott, A.; Ryder, K.; Gaines, L.; Anderson, P. Recycling Lithium-Ion Batteries from Electric Vehicles. *Nature* **2019**, *575*, 75−86.

(5) Xie, J.; Lu, Y.-C. A Retrospective on Lithium-Ion Batteries. *Nat. Commun.* **2020**, *11*, 2499.

(6) Grey, C. P.; Hall, D. S. Prospects for Lithium-Ion Batteries and Beyond—A 2030 Vision. *Nat. Commun.* **2020**, *11*, 6279.

(7) Li, M.; Lu, J.; Chen, Z.; Amine, K. 30 Years of Lithium-Ion Batteries. *Adv. Mater.* **2018**, *30*, 1800561.

(8) Palacín, M. R.; de Guibert, A. Why Do Batteries Fail? *Science* **2016**, *351*, 1253292.

(9) Larcher, D.; Tarascon, J. M. Towards Greener and More Sustainable Batteries for Electrical Energy Storage. *Nat. Chem.* **2015**, *7*, 19−29.

(10) Patel, M.; Mishra, K.; Banerjee, R.; Chaudhari, J.; Kanchan, D. K.; Kumar, D. Fundamentals, Recent Developments and Prospects of Lithium and Non-Lithium Electrochemical Rechargeable Battery Systems. *J. Energy Chem.* **2023**, *81*, 221−259.

(11) Guo, Y.; Li, H.; Zhai, T. Reviving Lithium-Metal Anodes for Next-Generation High-Energy Batteries. *Adv. Mater.* **2017**, *29*, 1700007.

(12) Liu, B.; Zhang, J.-G.; Xu, W. Advancing Lithium Metal Batteries. *Joule* **2018**, *2*, 833−845.

(13) Zhang, L.; Zhu, C.; Yu, S.; Ge, D.; Zhou, H. Status and Challenges Facing Representative Anode Materials for Rechargeable Lithium Batteries. *J. Energy Chem.* **2022**, *66*, 260−294.

(14) Zhang, J.-G.; Xu, W.; Xiao, J.; Cao, X.; Liu, J. Lithium Metal Anodes with Nonaqueous Electrolytes. *Chem. Rev.* **2020**, *120*, 13312−13348.

(15) Luo, Z.; Qiu, X.; Liu, C.; Li, S.; Wang, C.; Zou, G.; Hou, H.; Ji, X. Interfacial Challenges Towards Stable Li Metal Anode. *Nano Energy* **2021**, *79*, 105507.

(16) Wang, R.; Cui, W.; Chu, F.; Wu, F. Lithium Metal Anodes: Present and Future. *J. Energy Chem.* **2020**, *48*, 145−159.

(17) Chen, S.; Zheng, J.; Mei, D.; Han, K. S.; Engelhard, M. H.; Zhao, W.; Xu, W.; Liu, J.; Zhang, J.-G. High-Voltage Lithium-Metal Batteries Enabled by Localized High-Concentration Electrolytes. *Adv. Mater.* **2018**, *30*, 1706102.

(18) Ren, X.; Chen, S.; Lee, H.; Mei, D.; Engelhard, M. H.; Burton, S. D.; Zhao, W.; Zheng, J.; Li, Q.; Ding, M. S.; Schroeder, M.; Alvarado, J.; Xu, K.; Meng, Y. S.; Liu, J.; Zhang, J.-G.; Xu, W. Localized High-Concentration Sulfone Electrolytes for High-Efficiency Lithium-Metal Batteries. *Chem.* **2018**, *4*, 1877−1892.

(19) He, X.; Bresser, D.; Passerini, S.; Baakes, F.; Krewer, U.; Lopez, J.; Mallia, C. T.; Shao-Horn, Y.; Cekic-Laskovic, I.; Wiemers-Meyer, S.; Soto, F. A.; Ponce, V.; Seminario, J. M.; Balbuena, P. B.; Jia, H.; Xu, W.; Xu, Y.; Wang, C.; Horstmann, B.; Amine, R.; Su, C.-C.; Shi, J.; Amine, K.; Winter, M.; Latz, A.; Kostecki, R. The Passivity of Lithium

Electrodes in Liquid Electrolytes for Secondary Batteries. *Nat. Rev. Mater.* **2021**, *6*, 1036−1052.
(20) Zhao, H.; Wang, J.; Shao, H.; Xu, K.; Deng, Y. Gas Generation Mechanism in Li-Metal Batteries. *Energy Environ. Mater.* **2022**, *5*, 327−336.
(21) Chen, X.; Shen, X.; Li, B.; Peng, H.-J.; Cheng, X.-B.; Li, B.-Q.; Zhang, X.-Q.; Huang, J.-Q.; Zhang, Q. Ion-Solvent Complexes Promote Gas Evolution from Electrolytes on a Sodium Metal Anode. *Angew. Chem., Int. Ed.* **2018**, *57*, 734−737.
(22) Zhai, P.; Liu, L.; Gu, X.; Wang, T.; Gong, Y. Interface Engineering for Lithium Metal Anodes in Liquid Electrolyte. *Adv. Energy Mater.* **2020**, *10*, 2001257.
(23) Yang, H.; Li, J.; Sun, Z.; Fang, R.; Wang, D.-W.; He, K.; Cheng, H.-M.; Li, F. Reliable Liquid Electrolytes for Lithium Metal Batteries. *Energy Storage Mater.* **2020**, *30*, 113−129.
(24) Lin, D.; Liu, Y.; Cui, Y. Reviving the Lithium Metal Anode for High-Energy Batteries. *Nat. Nanotechnol.* **2017**, *12*, 194−206.
(25) Li, F.; Liu, J.; He, J.; Hou, Y.; Wang, H.; Wu, D.; Huang, J.; Ma, J. Additive-Assisted Hydrophobic Li^+-Solvated Structure for Stabilizing Dual Electrode Electrolyte Interphases through Suppressing $LiPF_6$ Hydrolysis. *Angew. Chem., Int. Ed.* **2022**, *61*, 202205091.
(26) Qi, S.; Wang, H.; He, J.; Liu, J.; Cui, C.; Wu, M.; Li, F.; Feng, Y.; Ma, J. Electrolytes Enriched by Potassium Perfluorinated Sulfonates for Lithium Metal Batteries. *Sci. Bull.* **2021**, *66*, 685−693.
(27) Haregewoin, A. M.; Wotango, A. S.; Hwang, B.-J. Electrolyte Additives for Lithium Ion Battery Electrodes: Progress and Perspectives. *Energy Environ. Sci.* **2016**, *9*, 1955−1988.
(28) Chen, X.; Zhang, Q. Atomic Insights into the Fundamental Interactions in Lithium Battery Electrolytes. *Acc. Chem. Res.* **2020**, *53*, 1992−2002.
(29) Chen, X.; Li, H. R.; Shen, X.; Zhang, Q. The Origin of the Reduced Reductive Stability of Ion-Solvent Complexes on Alkali and Alkaline Earth Metal Anodes. *Angew. Chem., Int. Ed.* **2018**, *57*, 16643−16647.
(30) Chen, X.; Shen, X.; Hou, T.-Z.; Zhang, R.; Peng, H.-J.; Zhang, Q. Ion−Solvent Chemistry-Inspired Cation-Additive Strategy to Stabilize Electrolytes for Sodium−Metal Batteries. *Chem.* **2020**, *6*, 2242−2256.
(31) Chen, X.; Yao, N.; Zeng, B.-S.; Zhang, Q. Ion−Solvent Chemistry in Lithium Battery Electrolytes: From Mono−Solvent to Multi−Solvent Complexes. *Fundam. Res.* **2021**, *1*, 393−398.
(32) Chen, X.; Liu, X.; Shen, X.; Zhang, Q. Applying Machine Learning to Rechargeable Batteries: From the Microscale to the Macroscale. *Angew. Chem., Int. Ed.* **2021**, *60*, 24354−24366.
(33) Yao, N.; Chen, X.; Fu, Z. H.; Zhang, Q. Applying Classical, *Ab Initio*, and Machine-Learning Molecular Dynamics Simulations to the Liquid Electrolyte for Rechargeable Batteries. *Chem. Rev.* **2022**, *122*, 10970−11021.
(34) Kim, S. C.; Oyakhire, S. T.; Athanitis, C.; Wang, J.; Zhang, Z.; Zhang, W.; Boyle, D. T.; Kim, M. S.; Yu, Z.; Gao, X.; Sogade, T.; Wu, E.; Qin, J.; Bao, Z.; Bent, S. F.; Cui, Y. Data-Driven Electrolyte Design for Lithium Metal Anodes. *Proc. Natl. Acad. Sci. U.S.A.* **2023**, *120*, No. e2214357120.
(35) Liu, Y.; Guo, B.; Zou, X.; Li, Y.; Shi, S. Machine Learning Assisted Materials Design and Discovery for Rechargeable Batteries. *Energy Storage Mater.* **2020**, *31*, 434−450.
(36) Lombardo, T.; Duquesnoy, M.; El-Bouysidy, H.; Årén, F.; Gallo-Bueno, A.; Jørgensen, P. B.; Bhowmik, A.; Demortière, A.; Ayerbe, E.; Alcaide, F.; Reynaud, M.; Carrasco, J.; Grimaud, A.; Zhang, C.; Vegge, T.; Johansson, P.; Franco, A. A. Artificial Intelligence Applied to Battery Research: Hype or Reality? *Chem. Rev.* **2022**, *122*, 10899−10969.
(37) Honrao, S. J.; Yang, X.; Radhakrishnan, B.; Kuwata, S.; Komatsu, H.; Ohma, A.; Sierhuis, M.; Lawson, J. W. Discovery of Novel Li SSE and Anode Coatings Using Interpretable Machine Learning and High-Throughput Multi-Property Screening. *Sci. Rep.* **2021**, *11*, 16484.
(38) Zhang, X.; Zhou, J.; Lu, J.; Shen, L. Interpretable Learning of Voltage for Electrode Design of Multivalent Metal-Ion Batteries. *npj Comput. Mater.* **2022**, *8*, 175.
(39) Chen, H.; Covert, I. C.; Lundberg, S. M.; Lee, S.-I. Algorithms to Estimate Shapley Value Feature Attributions. *Nat. Mach. Intell.* **2023**, *5*, 590−601.
(40) Laatifi, M.; Douzi, S.; Ezzine, H.; Asry, C. E.; Naya, A.; Bouklouze, A.; Zaid, Y.; Naciri, M. Explanatory Predictive Model for Covid-19 Severity Risk Employing Machine Learning, Shapley Addition, and Lime. *Sci. Rep.* **2023**, *13*, 5481.
(41) Yu, Z.; Wang, H.; Kong, X.; Huang, W.; Tsao, Y.; Mackanic, D. G.; Wang, K.; Wang, X.; Huang, W.; Choudhury, S.; Zheng, Y.; Amanchukwu, C. V.; Hung, S. T.; Ma, Y.; Lomeli, E. G.; Qin, J.; Cui, Y.; Bao, Z. Molecular Design for Electrolyte Solvents Enabling Energy-Dense and Long-Cycling Lithium Metal Batteries. *Nat. Energy* **2020**, *5*, 526−533.
(42) Wang, H.; Yu, Z.; Kong, X.; Huang, W.; Zhang, Z.; Mackanic, D. G.; Huang, X.; Qin, J.; Bao, Z.; Cui, Y. Dual-Solvent Li-Ion Solvation Enables High-Performance Li-Metal Batteries. *Adv. Mater.* **2021**, *33*, 2008619.
(43) Hou, L.-P.; Li, Z.; Yao, N.; Bi, C.-X.; Li, B.-Q.; Chen, X.; Zhang, X.-Q.; Zhang, Q. Weakening the Solvating Power of Solvents to Encapsulate Lithium Polysulfides Enables Long-Cycling Lithium−Sulfur Batteries. *Adv. Mater.* **2022**, *34*, 2270312.
(44) Liu, J.; Bao, Z.; Cui, Y.; Dufek, E. J.; Goodenough, J. B.; Khalifah, P.; Li, Q.; Liaw, B. Y.; Liu, P.; Manthiram, A.; Meng, Y. S.; Subramanian, V. R.; Toney, M. F.; Viswanathan, V. V.; Whittingham, M. S.; Xiao, J.; Xu, W.; Yang, J.; Yang, X.-Q.; Zhang, J.-G. Pathways for Practical High-Energy Long-Cycling Lithium Metal Batteries. *Nat. Energy* **2019**, *4*, 180−186.
(45) Xu, K. Li-Ion Battery Electrolytes. *Nat. Energy* **2021**, *6*, 763.
(46) Winter, M.; Barnett, B.; Xu, K. Before Li Ion Batteries. *Chem. Rev.* **2018**, *118*, 11433−11456.
(47) Xu, K. Electrolytes and Interphases in Li-Ion Batteries and Beyond. *Chem. Rev.* **2014**, *114*, 11503−11618.
(48) Rogers, D.; Hahn, M. Extended-Connectivity Fingerprints. *J. Chem. Inf. Model.* **2010**, *50*, 742−754.
(49) Laurens, V. D. M.; Hinton, G. Visualizing Data Using t-SNE. *J. Mach. Learn. Res.* **2008**, *9*, 2579−2605.
(50) Zhang, Q.-K.; Zhang, X.-Q.; Wan, J.; Yao, N.; Song, T.-L.; Xie, J.; Hou, L.-P.; Zhou, M.-Y.; Chen, X.; Li, B.-Q.; Wen, R.; Peng, H.-J.; Zhang, Q.; Huang, J.-Q. Homogeneous and Mechanically Stable Solid-Electrolyte Interphase Enabled by Trioxane-Modulated Electrolytes for Lithium Metal Batteries. *Nat. Energy* **2023**, *8*, 725−735.
(51) Yao, Y.-X.; Chen, X.; Yan, C.; Zhang, X.-Q.; Cai, W.-L.; Huang, J.-Q.; Zhang, Q. Regulating Interfacial Chemistry in Lithium-Ion Batteries by a Weakly Solvating Electrolyte. *Angew. Chem., Int. Ed.* **2021**, *60*, 4090−4097.

https://doi.org/10.1021/jacs.3c08346
J. Am. Chem. Soc. 2023, 145, 23764−23770